Physics Letters B 744 (2015) 250–259

Contents lists available at ScienceDirect

Physics Letters B

www.elsevier.com/locate/physletb

Collins and Sivers asymmetries in muonproduction of pions and kaons off transversely polarised protons

C. Adolph [h], R. Akhunzyanov [g], M.G. Alexeev [aa], G.D. Alexeev [g], A. Amoroso [aa,ac], V. Andrieux [v], V. Anosov [g], A. Austregesilo [j,q], B. Badełek [ae], F. Balestra [aa,ac], J. Barth [d], G. Baum [a], R. Beck [c], Y. Bedfer [v], A. Berlin [b], J. Bernhard [m], K. Bicker [j,q], E.R. Bielert [j], J. Bieling [d], R. Birsa [y], J. Bisplinghoff [c], M. Bodlak [s], M. Boer [v], P. Bordalo [l,1], F. Bradamante [x,y], C. Braun [h], A. Bressan [x,y,*], M. Büchele [i], E. Burtin [v], L. Capozza [v], M. Chiosso [aa,ac], S.U. Chung [q,2], A. Cicuttin [z,y], M.L. Crespo [z,y], Q. Curiel [v], S. Dalla Torre [y], S.S. Dasgupta [f], S. Dasgupta [x,y], O.Yu. Denisov [ac], S.V. Donskov [u], N. Doshita [ag], V. Duic [x], W. Dünnweber [p], M. Dziewiecki [af], A. Efremov [g], C. Elia [x,y], P.D. Eversheim [c], W. Eyrich [h], M. Faessler [p], A. Ferrero [v], M. Finger [s], M. Finger Jr. [s], H. Fischer [i], C. Franco [l], N. du Fresne von Hohenesche [m,j], J.M. Friedrich [q], V. Frolov [j], F. Gautheron [b], O.P. Gavrichtchouk [g], S. Gerassimov [o,q], R. Geyer [p], I. Gnesi [aa,ac], B. Gobbo [y], S. Goertz [d], M. Gorzellik [i], S. Grabmüller [q], A. Grasso [aa,ac], B. Grube [q], T. Grussenmeyer [i], A. Guskov [g], F. Haas [q], D. von Harrach [m], D. Hahne [d], R. Hashimoto [ag], F.H. Heinsius [i], F. Herrmann [i], F. Hinterberger [c], Ch. Höppner [q], N. Horikawa [r,4], N. d'Hose [v], S. Huber [q], S. Ishimoto [ag,5], A. Ivanov [g], Yu. Ivanshin [g], T. Iwata [ag], R. Jahn [c], V. Jary [t], P. Jasinski [m], P. Jörg [i], R. Joosten [c], E. Kabuß [m], B. Ketzer [q,6], G.V. Khaustov [u], Yu.A. Khokhlov [u,7], Yu. Kisselev [g], F. Klein [d], K. Klimaszewski [ad], J.H. Koivuniemi [b], V.N. Kolosov [u], K. Kondo [ag], K. Königsmann [i], I. Konorov [o,q], V.F. Konstantinov [u], A.M. Kotzinian [aa,ac], O. Kouznetsov [g], M. Krämer [q], Z.V. Kroumchtein [g], N. Kuchinski [g], F. Kunne [v,**], K. Kurek [ad], R.P. Kurjata [af], A.A. Lednev [u], A. Lehmann [h], M. Levillain [v], S. Levorato [y], J. Lichtenstadt [w], A. Maggiora [ac], A. Magnon [v], N. Makke [x,y], G.K. Mallot [j], C. Marchand [v], A. Martin [x,y,**], J. Marzec [af], J. Matousek [s], H. Matsuda [ag], T. Matsuda [n], G. Meshcheryakov [g], W. Meyer [b], T. Michigami [ag], Yu.V. Mikhailov [u], Y. Miyachi [ag], A. Nagaytsev [g], T. Nagel [q], F. Nerling [m], S. Neubert [q], D. Neyret [v], J. Novy [t], W.-D. Nowak [i], A.S. Nunes [l], A.G. Olshevsky [g], I. Orlov [g], M. Ostrick [m], R. Panknin [d], D. Panzieri [ab,ac], B. Parsamyan [aa,ac], S. Paul [q], G. Pesaro [x,y], D.V. Peshekhonov [g], S. Platchkov [v], J. Pochodzalla [m], V.A. Polyakov [u], J. Pretz [d,8], M. Quaresma [l], C. Quintans [l], S. Ramos [l,1], C. Regali [i], G. Reicherz [b], E. Rocco [j], N.S. Rossiyskaya [g], D.I. Ryabchikov [u], A. Rychter [af], V.D. Samoylenko [u], A. Sandacz [ad], S. Sarkar [f], I.A. Savin [g], G. Sbrizzai [x,y], P. Schiavon [x,y], C. Schill [i], T. Schlüter [p], K. Schmidt [i,3], H. Schmieden [d], K. Schönning [j], S. Schopferer [i], M. Schott [j], O.Yu. Shevchenko [g,19], L. Silva [l], L. Sinha [f], S. Sirtl [i], M. Slunecka [g], S. Sosio [aa,ac], F. Sozzi [y], A. Srnka [e], L. Steiger [y], M. Stolarski [l], M. Sulc [k], R. Sulej [ad], H. Suzuki [ag,4], A. Szabelski [ad], T. Szameitat [i,3], P. Sznajder [ad], S. Takekawa [aa,ac], J. ter Wolbeek [i,3], S. Tessaro [y], F. Tessarotto [y], F. Thibaud [v], S. Uhl [q], I. Uman [p], M. Virius [t], L. Wang [b], T. Weisrock [m], M. Wilfert [m], R. Windmolders [d], H. Wollny [v], K. Zaremba [af], M. Zavertyaev [o], E. Zemlyanichkina [g], M. Ziembicki [af], A. Zink [h]

* Corresponding author at: Department of Physics, University of Trieste, via A. Valerio 2, 34127 Trieste, ITALY.
** Corresponding authors.

http://dx.doi.org/10.1016/j.physletb.2015.03.056

[a] Universität Bielefeld, Fakultät für Physik, 33501 Bielefeld, Germany [9]
[b] Universität Bochum, Institut für Experimentalphysik, 44780 Bochum, Germany [9,16]
[c] Universität Bonn, Helmholtz-Institut für Strahlen- und Kernphysik, 53115 Bonn, Germany [9]
[d] Universität Bonn, Physikalisches Institut, 53115 Bonn, Germany [9]
[e] Institute of Scientific Instruments, AS CR, 61264 Brno, Czech Republic [10]
[f] Matrivani Institute of Experimental Research & Education, Calcutta-700 030, India [11]
[g] Joint Institute for Nuclear Research, 141980 Dubna, Moscow Region, Russia [12]
[h] Universität Erlangen–Nürnberg, Physikalisches Institut, 91054 Erlangen, Germany [9]
[i] Universität Freiburg, Physikalisches Institut, 79104 Freiburg, Germany [9,16]
[j] CERN, 1211 Geneva 23, Switzerland
[k] Technical University in Liberec, 46117 Liberec, Czech Republic [10]
[l] LIP, 1000-149 Lisbon, Portugal [13]
[m] Universität Mainz, Institut für Kernphysik, 55099 Mainz, Germany [9]
[n] University of Miyazaki, Miyazaki 889-2192, Japan [14]
[o] Lebedev Physical Institute, 119991 Moscow, Russia
[p] Ludwig-Maximilians-Universität München, Department für Physik, 80799 Munich, Germany [9,15]
[q] Technische Universität München, Physik Department, 85748 Garching, Germany [9,15]
[r] Nagoya University, 464 Nagoya, Japan [14]
[s] Charles University in Prague, Faculty of Mathematics and Physics, 18000 Prague, Czech Republic [10]
[t] Czech Technical University in Prague, 16636 Prague, Czech Republic [10]
[u] State Scientific Center Institute for High Energy Physics of National Research Center 'Kurchatov Institute', 142281 Protvino, Russia
[v] CEA IRFU/SPhN Saclay, 91191 Gif-sur-Yvette, France [16]
[w] Tel Aviv University, School of Physics and Astronomy, 69978 Tel Aviv, Israel [17]
[x] University of Trieste, Department of Physics, 34127 Trieste, Italy
[y] Trieste Section of INFN, 34127 Trieste, Italy
[z] Abdus Salam ICTP, 34151 Trieste, Italy
[aa] University of Turin, Department of Physics, 10125 Turin, Italy
[ab] University of Eastern Piedmont, 15100 Alessandria, Italy
[ac] Torino Section of INFN, 10125 Turin, Italy
[ad] National Centre for Nuclear Research, 00-681 Warsaw, Poland [18]
[ae] University of Warsaw, Faculty of Physics, 02-093 Warsaw, Poland [18]
[af] Warsaw University of Technology, Institute of Radioelectronics, 00-665 Warsaw, Poland [18]
[ag] Yamagata University, Yamagata, 992-8510, Japan [14]

ARTICLE INFO

Article history:
Received 21 August 2014
Received in revised form 24 March 2015
Accepted 26 March 2015
Available online 1 April 2015
Editor: M. Doser

ABSTRACT

Measurements of the Collins and Sivers asymmetries for charged pions and charged and neutral kaons produced in semi-inclusive deep-inelastic scattering of high energy muons off transversely polarised protons are presented. The results were obtained using all the available COMPASS proton data, which were taken in the years 2007 and 2010. The Collins asymmetries exhibit in the valence region a non-zero signal for pions and there are hints of non-zero signal also for kaons. The Sivers asymmetries are found to be positive for positive pions and kaons and compatible with zero otherwise.

1. Introduction

The description of the nucleon spin structure is still one of the open issues in hadron physics. In the last decades major progress in this field has been made by an interplay between new experimental results and the development of non-collinear QCD. The first information on transverse spin and transverse momentum effects have become available recently. Presently, the complete description of quarks in the nucleon includes all possible correlations between quark spin, quark transverse momentum and nucleon spin [1,2]. At leading twist, these correlations are described for each quark flavour by eight transverse momentum dependent (TMD) parton distribution functions (PDFs). After integration over transverse momentum, only three of them survive, namely the number density, the helicity and the transversity PDFs. One way to access experimentally these TMD PDFs is via semi-inclusive lepton–nucleon deep inelastic scattering (SIDIS), i.e. by studying deep-inelastic

E-mail addresses: Andrea.Bressan@cern.ch (A. Bressan), Fabienne.Kunne@cern.ch (F. Kunne), Anna.Martin@ts.infn.it (A. Martin).

[1] Also at Instituto Superior Técnico, Universidade de Lisboa, Lisbon, Portugal.
[2] Also at Department of Physics, Pusan National University, Busan 609-735, Republic of Korea and at Physics Department, Brookhaven National Laboratory, Upton, NY 11973, USA.
[3] Supported by the DFG Research Training Group Programme 1102 "Physics at Hadron Accelerators".
[4] Also at Chubu University, Kasugai, Aichi 487-8501, Japan. See footnote 14.
[5] Also at KEK, 1-1 Oho, Tsukuba, Ibaraki 305-0801, Japan.
[6] Present address: Universität Bonn, Helmholtz-Institut für Strahlen- und Kernphysik, 53115 Bonn, Germany.
[7] Also at Moscow Institute of Physics and Technology, Moscow Region, 141700, Russia.
[8] Present address: RWTH Aachen University, III. Physikalisches Institut, 52056 Aachen, Germany.
[9] Supported by the German Bundesministerium für Bildung und Forschung.
[10] Supported by Czech Republic MEYS Grants ME492 and LA242.
[11] Supported by SAIL (CSR), Govt. of India.
[12] Supported by CERN-RFBR Grants 08-02-91009 and 12-02-91500.
[13] Supported by the Portuguese FCT – Fundação para a Ciência e Tecnologia, COMPETE and QREN, Grants CERN/FP/109323/2009, CERN/FP/116376/2010 and CERN/FP/123600/2011.
[14] Supported by the MEXT and the JSPS under the Grants No. 18002006, No. 20540299 and No. 18540281; Daiko Foundation and Yamada Foundation.
[15] Supported by the DFG cluster of excellence 'Origin and Structure of the Universe' (www.universe-cluster.de).
[16] Supported by EU FP7 (HadronPhysics3, Grant Agreement number 283286).
[17] Supported by the Israel Science Foundation, founded by the Israel Academy of Sciences and Humanities.
[18] Supported by the Polish NCN Grant DEC-2011/01/M/ST2/02350.
[19] Deceased.

scattering (DIS) with detection of at least one of the produced hadrons. When the target nucleon is transversely polarised, the SIDIS cross section exhibits different azimuthal modulations [3] in different combinations of the two angles ϕ_S and ϕ_h. These are the azimuthal angles of the initial nucleon transverse spin vector and of the produced hadron momentum in a reference system, in which the z-axis is the virtual photon direction and the x–z plane is the lepton plane according to Ref. [4]. The amplitudes of the modulations in the cross section (the so-called transverse spin asymmetries) are proportional to convolutions of TMD PDFs with TMD fragmentation functions. The two most thoroughly studied transverse spin asymmetries are the Collins and Sivers asymmetries. The Collins asymmetries allow access to the transversity PDFs coupled to the Collins fragmentation functions [5]. The Sivers asymmetries give access to the Sivers PDFs [6], which describe the correlations between quark transverse momentum and nucleon spin. A Sivers PDF always appears in combination with an 'ordinary' (unpolarised) fragmentation function that describes the fragmentation of a quark into a hadron.

In this paper, we present results on the Collins and Sivers asymmetries for pions and kaons produced on transversely polarised protons in a NH_3 target. Such measurements are in line with the set of measurements done by the COMPASS Collaboration in the last years. Results on polarised deuterons were obtained for unidentified hadrons [7], pions and kaons [8], and on polarised protons for charged unidentified hadrons [9–11]. The results presented in this Letter are extracted from all available COMPASS data taken in 2007 and 2010 using transversely polarised protons. For the measurements in 2007 and 2010, a similar spectrometer configuration was used. As compared to the measurements on transversely polarised deuterons, the measurements on transversely polarised protons benefit from a major upgrade of the apparatus performed in 2005. Of particular relevance for these measurements is the upgrade of the RICH detector [12], which led to improved efficiency and purity for the samples of identified particles, and the use of a new target solenoid magnet with a polar angle acceptance of 180 mrad as compared to the 70 mrad of the magnet used until 2005. Measurements of these asymmetries by the HERMES experiment exist [13,14] in a different kinematic range (measurements in a limited x range also exist on neutron targets, see [15–17]). Comparison with these results are also presented in the paper.

2. Apparatus and data selection

The COMPASS spectrometer [18] is in operation in the North Area of CERN since 2002. The μ^+ beam provided by the M2 beam line had a momentum of 160 GeV/c, a momentum spread $\Delta p/p = \pm 5\%$, and a longitudinal polarisation of -80% that originated from the π-decay mechanism. The mean beam intensity was about $2.3 \times 10^7 \mu^+/\text{s}$ and $4 \times 10^7 \mu^+/\text{s}$ with spill lengths of 4.8 s and 10 s in 2007 and 2010, respectively.

The target consisted of three cylindrical cells of 4 cm diameter, each separated by gaps of 5 cm. The length of the central cell was 60 cm and that of the two outer ones 30 cm. For the measurement of transverse spin effects, the target material was polarised along the vertical direction. In order to reduce systematic effects, neighbouring cells were polarised in opposite directions, which allows for simultaneous data taking with both target spin directions. To further minimise systematic effects, the polarisation of each cell was reversed every 4–5 days. During the 2007 data taking, a total amount of 12×10^9 events (440 TB) was recorded in six periods, each consisting of two sub-periods of data taking with opposite polarisation. In 2010 about 37×10^9 events (1.9 PB)of raw data were recorded over twelve periods.

Only events with a photon virtuality $Q^2 > 1$ (GeV/c)^2 and a mass of the hadronic final state $W > 5$ GeV/c^2 have been used to ensure the kinematic region of DIS. The upper limit on the fractional energy of the virtual photon (y) was set to 0.9 to reduce uncertainties due to electromagnetic radiative corrections and contamination from pion decay. A lower limit on y is required to ensure a good resolution in this variable. In the standard analysis this limit has been set to 0.1. A complementary sample with $0.05 < y < 0.1$ was also studied, mainly to address the Q^2 dependence of the asymmetries. The Bjorken variable x covers the range from 0.003 to 0.7. A minimum value of 0.1 GeV/c for the hadron transverse momentum p_T^h with respect to the virtual photon direction was required to ensure good resolution in the measured azimuthal angle. A minimum value for the relative hadron energy z with respect to the virtual photon energy is needed to select hadrons from the current fragmentation region. This value has been set to 0.2 for the standard sample, while a complementary lower-z region ($0.1 < z < 0.2$) was also studied.

The stability of the apparatus during data taking is crucial. Therefore, various tests were performed using the 2007 and 2010 data, as described in [9–11]. As a result from these quality tests, only four periods of data taking in 2007 were used for the analysis of the Sivers asymmetries, while for the Collins asymmetry all six periods were used. This can be understood as the Sivers asymmetry is very sensitive to instabilities in the spectrometer acceptance, because it represents the amplitude of the modulation that depends on the azimuthal angle of the hadron transverse momentum with respect to the target spin vector, which is aligned along a fixed direction. Due to improved detector stability, all periods of 2010 could be used for the extraction of both asymmetries.

3. Particle identification

3.1. Charged pions and kaons

The RICH detector information was used to identify charged hadrons as kaons and pions in the momentum range between the Cherenkov threshold (about 2.6 GeV/c for pions, 9 GeV/c for kaons) and 50 GeV/c. The detector after the upgrade of 2005 and the particle identification (PID) procedure are described in Ref. [19] and only the relevant details of the likelihood PID method are given here.

The pattern of the detected photons in each event is analysed taking into account the predicted path of the charged particle to compute likelihood values for each reconstructed track entering the RICH acceptance. The likelihood values are computed for different mass hypotheses ($\mathcal{L}_M$, with $M = \pi, K, p, e$) and for the hypothesis of absence of signal, namely the so-called background hypothesis ($\mathcal{L}_{back}$). A mass value is attributed to a track if the likelihood for the corresponding mass hypothesis is the largest. In addition, cuts on the ratio of the largest likelihood value to the second largest one are applied to minimise the misidentification probability. A specific cut on the ratio $\mathcal{L}_K/\mathcal{L}_{back}$ is applied to keep the contamination of protons in the kaon sample at a few percent in the momentum range between the kaon and the proton thresholds one (about 18 GeV/c). The cuts have been tuned to improve the particle identification efficiency and the sample purity (defined as the fraction of K (π) inside the identified K (π) sample) in order to maximise their product which is the figure of merit for particle identification. The tuning has been performed on the data collected in 2007 and, thanks to the high stability of the detector, the same cuts have been applied for the 2010 data.

The particle identification efficiencies and misidentification probabilities were determined using samples of pions from the K^0 decay and of kaons from the ϕ decay. The efficiencies are about

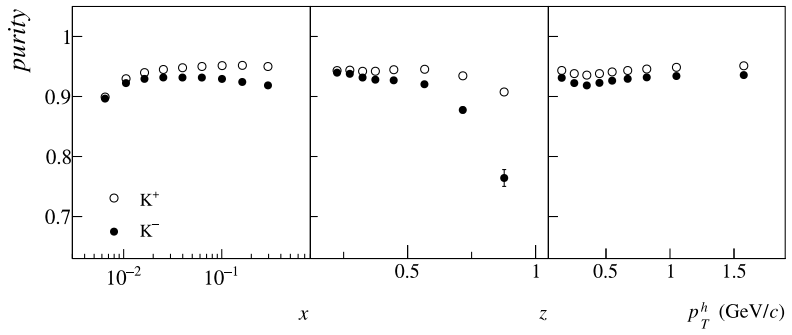

Fig. 1. Purity of the identified positive and negative kaons as a function of x, z, p_T^h.

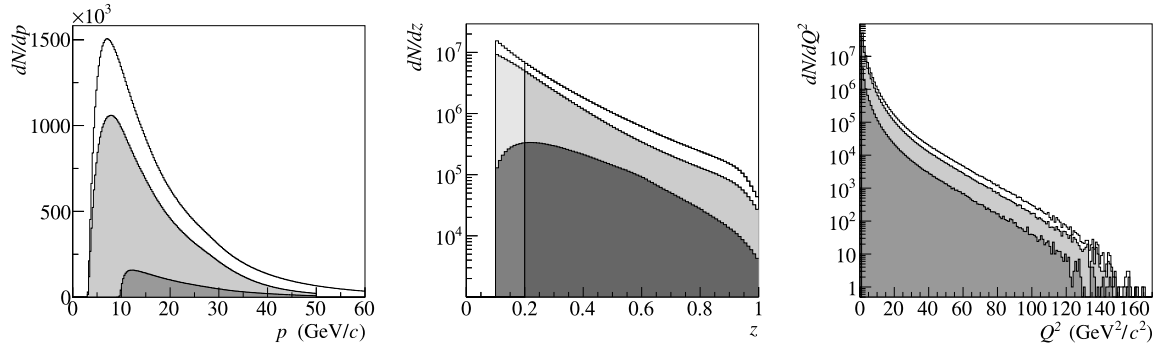

Fig. 2. Momentum p (left), relative energy z (centre), Q^2 (right) distribution of the unidentified charged hadrons (white), pions (light grey) and kaons (dark grey). The same code for particles, with slightly lighter gray tones is used for the $0.1 < z < 0.2$ kinematic interval; the standard selection is used for the kinematic distributions in x and Q^2.

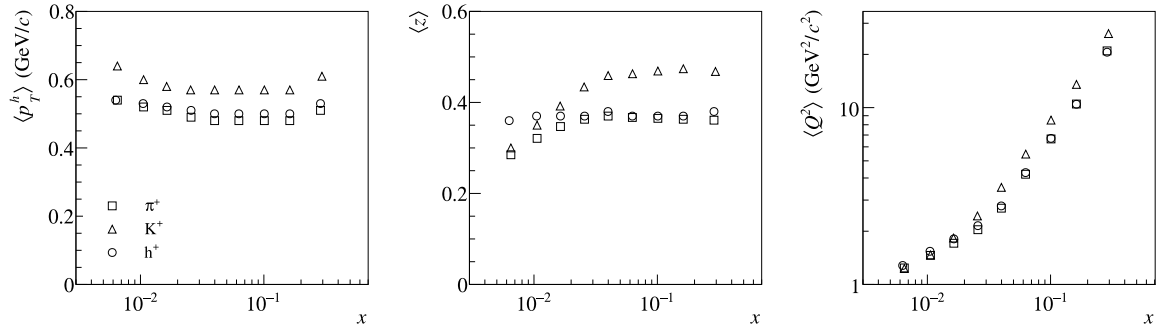

Fig. 3. Mean values of the transverse momentum p_T^h (left), relative energy z (centre), Q^2 (right) of the unidentified positive hadrons (circles), pions (squares) and kaons (triangles). The mean values for negative particles are essentially identical.

97% for pions and 94% for kaons. These values start to decrease for momenta about 30 GeV/c and reach values of 60% in the larger momentum region. In order to achieve high values of the sample purity, the misidentification probabilities between pions and kaons were kept as low as a few percent even at the largest momentum values, by adjusting the value of the cut on the ratio of the largest likelihood value to the second largest one. The purity depends also on the relative population of the various particle types and is evaluated from the particle identification efficiencies and misidentification probabilities and the number of identified kaons and pions for every bin in which the asymmetry are measured. The proton contribution is very small as already mentioned, and was neglected for the purity calculation. The average purity values for pions are above 99%. The kaon purity in the different x, z, and p_T^h bins is shown in Fig. 1. It is about 94% with a mostly mild dependence on the variables. The strongest dependence is visible in the large z region for the negative kaon sample, which is due to the increasing ratio of pions to kaons. Both the sample purity and the identification efficiency have been measured and found to be compatible in the two data taking years as well as in the different periods of each year. Effects due to the hadron identification using the RICH have been evaluated and found to be small with respect to the statistical uncertainties (less than half of the statistical uncertainties in the worst case, namely the last z bin). No correction has been applied to the final results and the estimates of the possible effects have been included in the systematic point-to-point uncertainties.

In Fig. 2 the distributions in momentum p, z and Q^2 for identified pions and kaons are shown and compared to those for unidentified hadrons. The clearly visible differences in the p and z distributions are due to the different momentum cuts required by the particle identification. The mean values of the p_T^h, z and Q^2 distributions as a function of x are shown in Fig. 3. The different x dependence of the mean values of z for the different particles is due to the different cuts in momentum combined with the x dependence of the kinematic correlation between z and p. The resulting statistics for charged pions and kaons after all cuts are shown in Table 1.

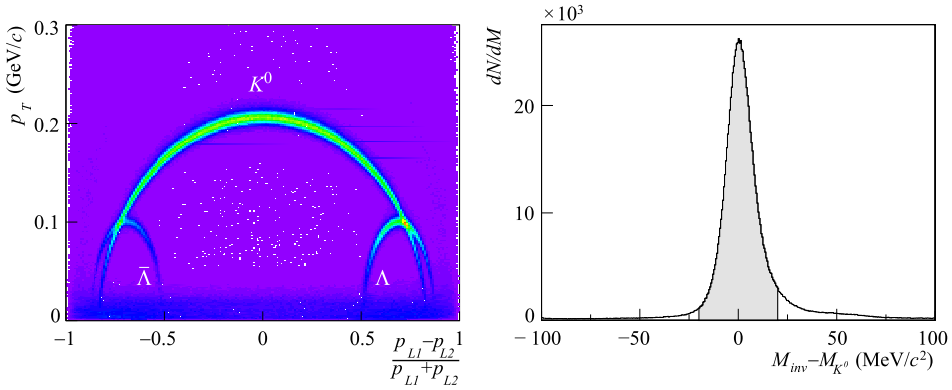

Fig. 4. Left: Armenteros–Podolansky plot of the hadron pair. Right: Difference of the invariant mass of the hadron pair and the PDG value of the K^0 mass. The mass range used for the analysis is shaded.

Table 1
Final statistics for 2007 and 2010 for identified charged pions and kaons and neutral kaons.

Year	Number of particles ($\times 10^{-6}$)				
	π^+	π^-	K^+	K^-	K^0
2007 (Collins)	10.77	9.41	1.79	1.10	0.37
2007 (Sivers)	6.84	5.97	1.12	0.69	0.25
2010	27.26	23.72	4.48	2.71	1.00

3.2. K^0 identification

The K^0 identification is based on the detection of two oppositely charged tracks coming from a secondary vertex, for which the 2-pion invariant mass lies in the window $m_{K^0} \pm 20$ MeV/c^2. A separation between the primary and the secondary vertex of at least 10 cm was required. Furthermore, the angle between the reconstructed momentum vector of the track pair and the vector connecting the primary and secondary vertices was required to be smaller than 10 mrad. On the left side of Fig. 4, the Armenteros–Podolansky plot of the hadron pair is shown, in which the transverse momentum p_T of one hadron with respect to the sum of hadron momenta is shown as a function of the difference of the longitudinal momenta over their sum, $(p_{L1} - p_{L2})/(p_{L1} + p_{L2})$. The K^0 band is clearly visible as well as the Λ and $\bar{\Lambda}$ bands. In order to exclude the contamination by the $\Lambda/\bar{\Lambda}$ signal, the p_T region between 80 MeV/c and 110 MeV/c was excluded. The background from e^+e^- pairs was suppressed by a lower cut on p_T at 40 MeV/c. For the detected K^0s, the difference between their mass value and the PDG [20] value is shown in the right panel of Fig. 4, where the vertical lines at ± 20 MeV/c^2 enclose the K^0s used for further analysis. The asymmetry in the background visible in the plot is a consequence of the p_T cut used to suppress the $\Lambda/\bar{\Lambda}$ contamination which reduces the ratio 'background to total' in the selected mass range from 0.07 to 0.02. The transverse spin asymmetries of the background have been checked to be compatible with zero and the overall effect on the final results have been evaluated to be completely negligible as compared to the statistical uncertainties. The same cuts on z and p_T^h as for the charged π and K samples were applied to the neutral kaons. The mean value of the relevant kinematic variables are very close to those for pions given in Fig. 3 and the final statistics for the K^0 sample are given in Table 1.

4. Results

In order to extract the transverse spin asymmetries from the data, the same procedure as described in Refs. [10,11] was used. The asymmetries were evaluated in bins of the kinematic variables x, z, or p_T^h, using the same binning as in our previous analyses [8]. All the numerical results are available on HEPDATA. The (ϕ_S, ϕ_h) distributions from the different target cells and subperiods were fitted using an extended maximum likelihood estimator [9], and the eight transverse spin asymmetries expected in the SIDIS process were extracted simultaneously. It has been checked that including in the fit possible additional terms due to the longitudinal components of the target polarisation [21], the changes in the resulting Sivers and Collins asymmetry values are negligible as compared to the statistical uncertainty. Note that the asymmetry reported here (one dimensional projection, integrated over the other kinematics variables) have in principle, the instrumental acceptance folded in. They are not corrected for it since in all our simulations the corrections turned out to be negligible.

The resulting $\sin(\phi_h + \phi_s)$ and $\sin(\phi_h - \phi_s)$ modulations yield the Collins and Sivers asymmetries, respectively, after division by *i*) the target material dilution factor f, *ii*) the average target proton polarisation, and for the Collins asymmetry *iii*) the transverse spin transfer coefficient. In addition to ammonia the target cells contain small amounts of other materials. The dilution factor takes into account that the selected sample does not only include scattering on the polarised protons but also on other nuclei (i.e. different isotopes of He and N), whose content inside the solid state target containers is known better than % level. As for all the other COMPASS results on spin dependent observables (see f.i. [22]), the dilution factor f is expressed in terms of the number n_A of nuclei with mass number A and the corresponding spin-independent cross sections σ_A^{tot} per nucleon (corrected for radiative effects) for all the elements involved $f = n_{\text{H}} \cdot \sigma_{\text{H}}^{\text{tot}} / (\Sigma_{\text{A}} n_{\text{A}} \cdot \sigma_{\text{A}}^{\text{tot}})$. The total cross section ratios, $\sigma_{\text{A}}^{\text{tot}}/\sigma_{\text{H}}^{\text{tot}}$, are obtained from the structure function ratios, $F_2^{\text{n}}(x,y)/F_2^{\text{p}}(x,y)$ and $F_2^{\text{A}}(x,y)/F_2^{\text{d}}(x,y)$ [23,24]. The original procedure leading from the measured cross section ratios $\sigma_A^{\text{tot}}/\sigma_H^{\text{tot}}$ to the published structure function ratios was inverted step by step involving the corrections to account for the non-isoscalar content of the target and the radiative corrections. For unmeasured nuclei the cross section ratios are obtained in the same way from a parameterisation of $F_2^{\text{A}}(x,y)/F_2^{\text{d}}(x,y)$ as a function of A. In the present analysis, the dilution factor is modified by a correction factor $\rho = \sigma_{\text{p}}^{1\gamma}/\sigma_{\text{p}}^{\text{tot}}$ accounting for the dilution due to radiative events on unpolarised protons [25]. Moreover a correction for polarisation of the admixture of ^{15}N to ^{14}N is also applied. The dilution factor is calculated in any bin and for every event using x and y. Its dependence on other kinematic variables, *e.g.* on p_T or z_h has been studied but no significant variation was observed at COMPASS energies. The resulting dilu-

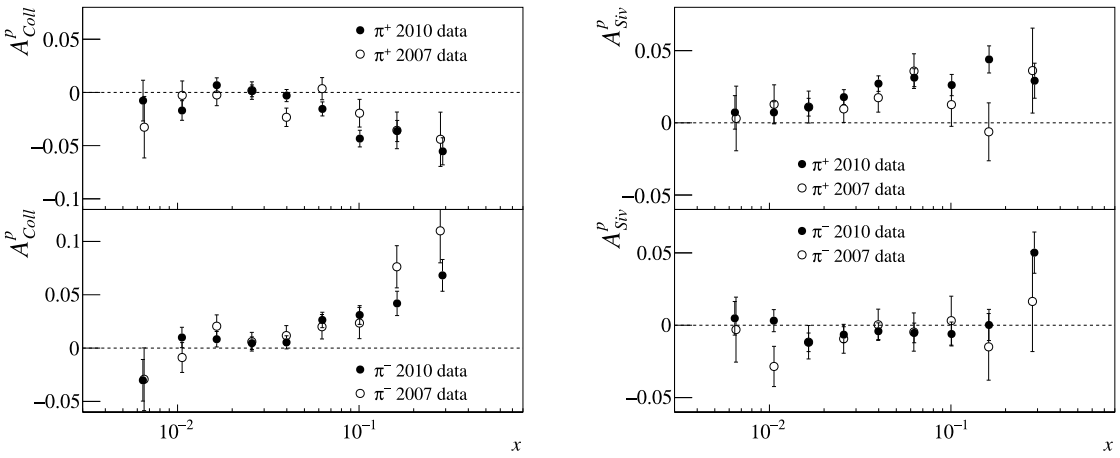

Fig. 5. Left: comparison between the Collins asymmetries for pions as a function of x, extracted from 2007 and 2010 data taking. Right: the same comparison for the Sivers asymmetries.

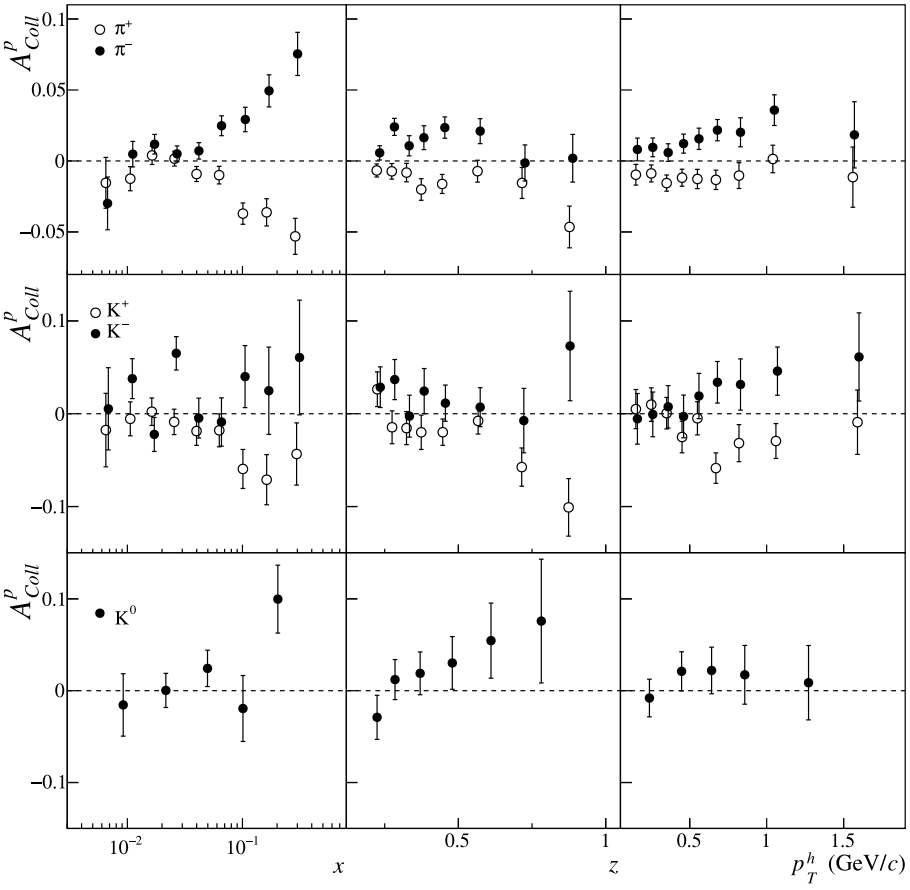

Fig. 6. The Collins asymmetries for charged pions (top), charged kaons (middle) and neutral kaons (bottom) on proton as a function of x, z and p_T^h.

tion factor increases with x from about 0.14 to 0.17. As a function of z and p_T^h it is almost constant with an average value of 0.15.

A non-flat azimuthal acceptance introduces correlations between the various modulations resulting from the fit. The correlation coefficients for Collins vs. Sivers asymmetries are found to be small and below 0.2 for all bins. Moreover, the asymmetries measured along different projections of the (x, z, p_T^h) phase space are statistically correlated, because the overall sample of events is the same. In the case of COMPASS, these correlation coefficients for the Collins and for the Sivers asymmetries are all smaller than about 0.3, but non-negligible, so that they should be taken into account in any global fit. They are slightly different for kaons and pions due to the different kinematic coverage of the two samples.

In order to estimate the systematic uncertainties, several tests were performed based on our previous work for the charged hadrons [9–11]. The effect of changes in the azimuthal acceptance between the data sets used to extract the asymmetries was quantified building false asymmetries, namely assuming a wrong polarisation direction in the target cells. The Collins and Sivers asymmetries were extracted splitting the data according to the scattered muon direction (up and down, left and right), and the statistical

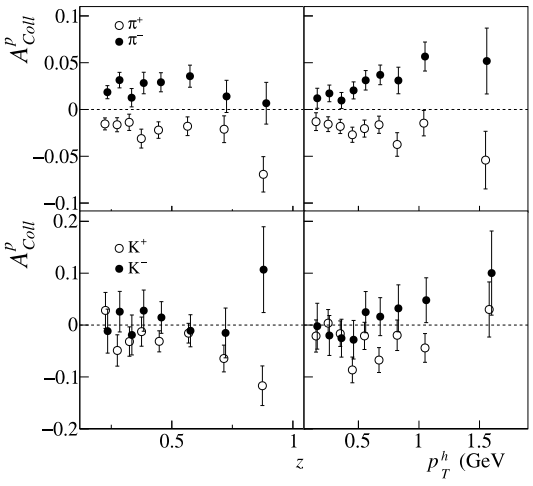

Fig. 7. The Collins asymmetries for pions (top) and kaons (bottom) as a function of z and p_T^h, requiring $x > 0.032$.

compatibility of the results was checked. No such false asymmetry was observed within the accuracy of the measurement and the point-to-point systematic uncertainties were evaluated from these tests as a fraction of the statistical error. For 2010, this fraction is 0.6 and for 2007 it ranges between 0.5 and 0.7. The systematic uncertainty due to particle misidentification is very small and included in these fractions. All results are subject to a 5% scale uncertainty that results from the uncertainties in the target polarisation and dilution factor.

For both years of data taking, the asymmetries were evaluated in each period and their compatibility was checked. While for 2010 this test shows good agreement among the results of the different periods, for 2007 it introduces an additional source of systematic uncertainties for the Sivers asymmetries. Very much like in the case of unidentified hadrons, an additional absolute uncertainty of ± 0.012 was assigned to the π^+ Sivers asymmetry. No such time dependence was observed either for the other hadrons or for the Collins asymmetries. This value is taken to be half of the difference between the mean asymmetries evaluated using the data from the beginning and the end of the 2007 data taking. Fig. 5 shows the Collins and Sivers asymmetries for pions as a function of x from the two data taking years, obtained as weighted mean of the asymmetries from the different periods. The two measurements are in good agreement for the pions and for the not shown kaons. The substantial improvement of the statistical precision of the 2010 data with respect to the 2007 data amounts to a factor of 1.6 for the Collins asymmetry and of 1.9 for the Sivers asymmetry. The final results were obtained combining the two samples, taking into account the different statistical and systematic uncertainties. The resulting systematic uncertainties are about 0.6 of the statistical ones for all the particle types.

The Collins asymmetries as a function of x, z, or p_T^h measured by COMPASS for pions and kaons on transversely polarised protons are shown in Fig. 6. The pion asymmetries are very similar to the unidentified hadron asymmetries [10]: at small x they are compatible with zero, while in the valence region they show an increasing signal, which has opposite sign for π^+ and π^-. This naively indicates that the unfavoured and favoured Collins fragmentation functions have opposite sign. The results for charged kaons, although with larger statistical uncertainties, show a similar trend: in particular the K^+ asymmetry has a negative trend with increasing x, and the K^- one is positive on average. The Collins asymmetry for neutral kaons shows a positive trend with increasing z. The average asymmetry is positive but compatible with zero within the statistical uncertainty. In order to investigate in more detail the behaviour of the asymmetries as a function of z and p_T^h, the asymmetries for charged hadrons were evaluated in a region where the signal is different from zero, namely $x > 0.032$. The results are shown in Fig. 7 for pions and kaons. They are in good agreement with the other existing measurements on a proton target from the HERMES experiment [13]. This is a non-obvious result, as in the last x bins the COMPASS Q^2 values are larger by a factor 3–4 than the HERMES ones. The weak Q^2 dependence of the Collins asymmetry is also supported by a recent global fit [26] of the HERMES pion results, the COMPASS preliminary pion asymmetries from the 2010 data, and the Belle [27] $e^+e^- \to \pi^+\pi^-$ asymmetries, which is able to provide a good description of all the data sets. A comparison between the final results of this paper and the fit is shown in Fig. 8.

The Collins asymmetry for charged hadrons was further investigated by extending the standard kinematic ranges in z and y. Compared to the above presented results, the asymmetries extracted in

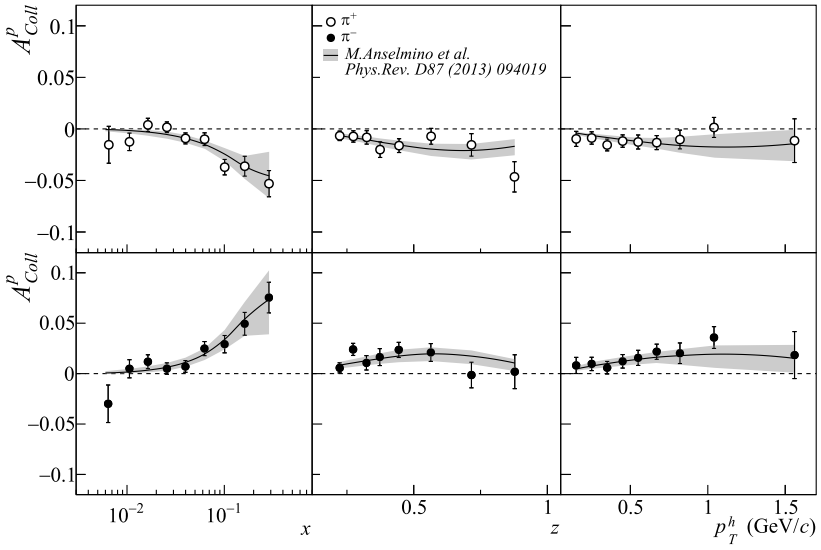

Fig. 8. Comparison between the Collins asymmetries for pions and one of the fits in [26] (fit with standard parameterisation and fit of A_{12} Belle asymmetries [27]). The preliminary asymmetries from 2010 data are included in the fit.

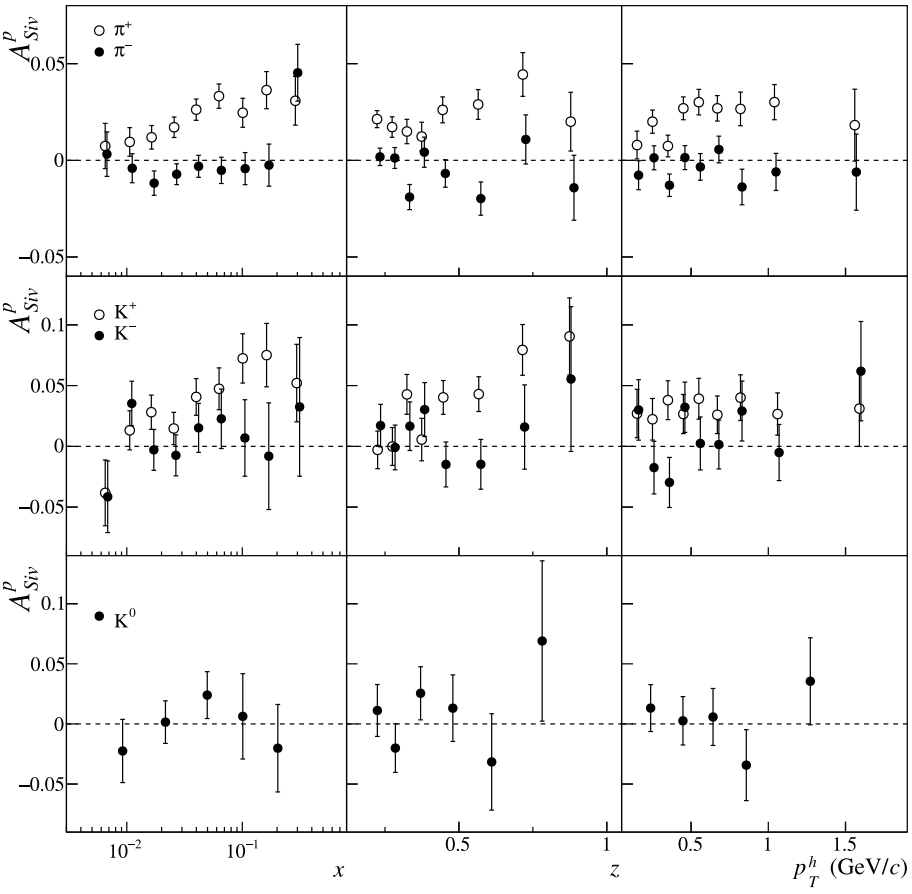

Fig. 9. The Sivers asymmetries for charged pions (top), charged kaons (middle) and neutral kaons (bottom) as a function of x, z and p_T^h.

the low-z region ($0.1 < z < 0.2$) gave no indication for a substantial z-dependence, neither for pions nor for kaons. Similarly, in the low-y region ($0.05 < y < 0.1$) the pion asymmetries do not exhibit any special behaviour, while the kaon ones suffer from too low statistics.

The Sivers asymmetries measured by COMPASS for pions and kaons on transversely polarised protons are shown in Fig. 9. Also in this case, the pion asymmetries are very similar to the unidentified hadron asymmetries [11]. The asymmetries for negative pions and kaons, as well as for neutral kaons are compatible with zero, while for positive pions and kaons there is a clear evidence for a positive signal extending over the full measured x region and increasing with z. Very intriguing is the fact that, as for HERMES [14], the K^+ signal is larger than the π^+ one, which indicates a possibly not negligible role of sea quarks [28–30]. This is well visible in Fig. 10, where the two asymmetries are directly compared, and from the mean values in the $x > 0.032$ region, which are respectively 0.027 ± 0.005 and 0.043 ± 0.014. Unlike the case of the Collins asymmetry, the Sivers asymmetry measured by COMPASS at large x for positive pions and kaons is smaller than the one from HERMES [14]. This difference is well visible also in the z and p_T^h variables when selecting the $x > 0.032$ region of the COMPASS data, as shown in Fig. 11. Several fits, which include the recently revisited Q^2 evolution, were performed using HERMES asymmetries [14], COMPASS asymmetries on deuteron [8] and for unidentified hadrons on proton [11], and JLab Hall A asymmetries on ^{3}He [15,16]. In Fig. 12, the results of some of these fits [31–33], which employ Q^2 TMD evolutions, are shown to well reproduce the COMPASS results. It will be interesting to see the results of such fits when the results presented in this Letter will be included.

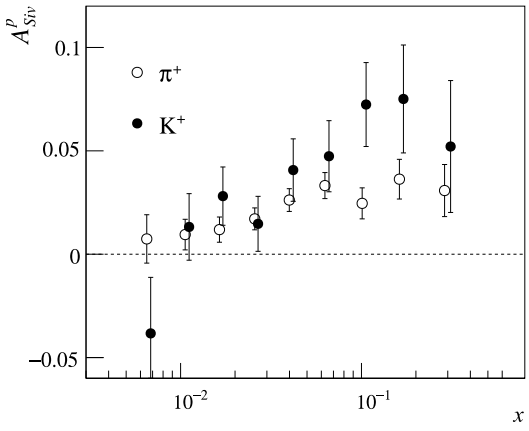

Fig. 10. The Sivers asymmetries for positive pions and kaons, as a function of x.

More information on the Q^2 evolution is provided by the study of the Sivers asymmetries in the low-y region between 0.05 and 0.1, performed only using the 2010 data (as already done for charged hadrons [10,11]). The pion asymmetries in this region are compared in the left panel of Fig. 13 to the asymmetries obtained in the standard y range. In the region of overlap the mean Q^2 values of these two samples are respectively 3.5 $(\mathrm{GeV}/c)^2$ and 1.8 $(\mathrm{GeV}/c)^2$. As for unidentified hadrons, there is an indication for an increase of the π^+ asymmetries at low-y. The dependence of the Sivers asymmetries with z is further investigated considering the z region between 0.1 and 0.2, where the asymmetries

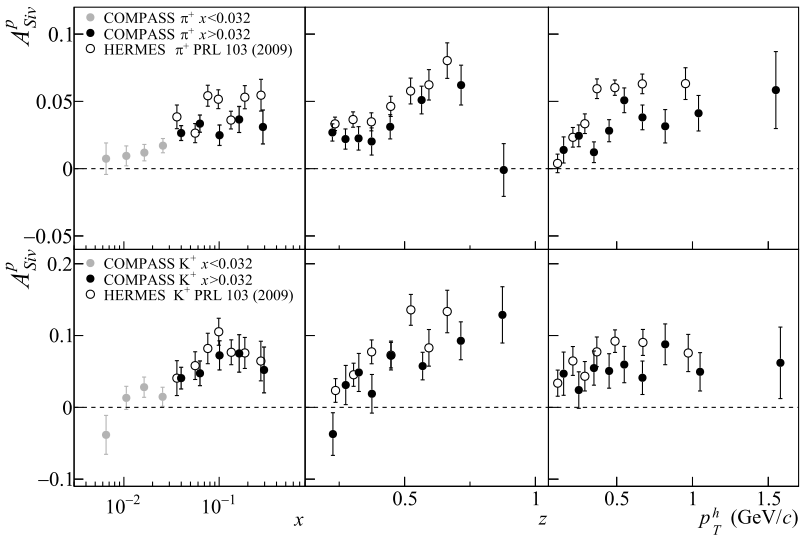

Fig. 11. The Sivers asymmetries for positive pions (top) and kaons (bottom) on proton as a function of x, z and p_T^h, requiring $x > 0.032$. The asymmetries are compared to HERMES results [14].

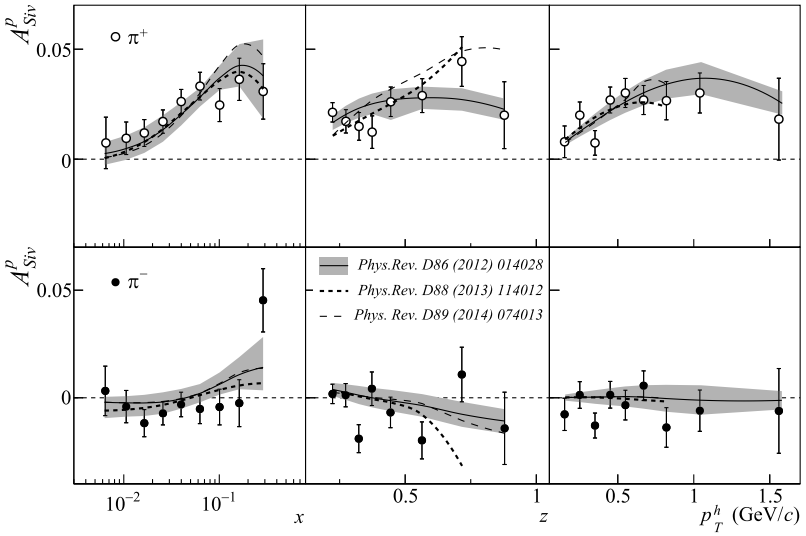

Fig. 12. Comparison between the Sivers asymmetries for pions and existing global fits [31–33], in which the COMPASS results for the unidentified hadrons on protons [11] are included.

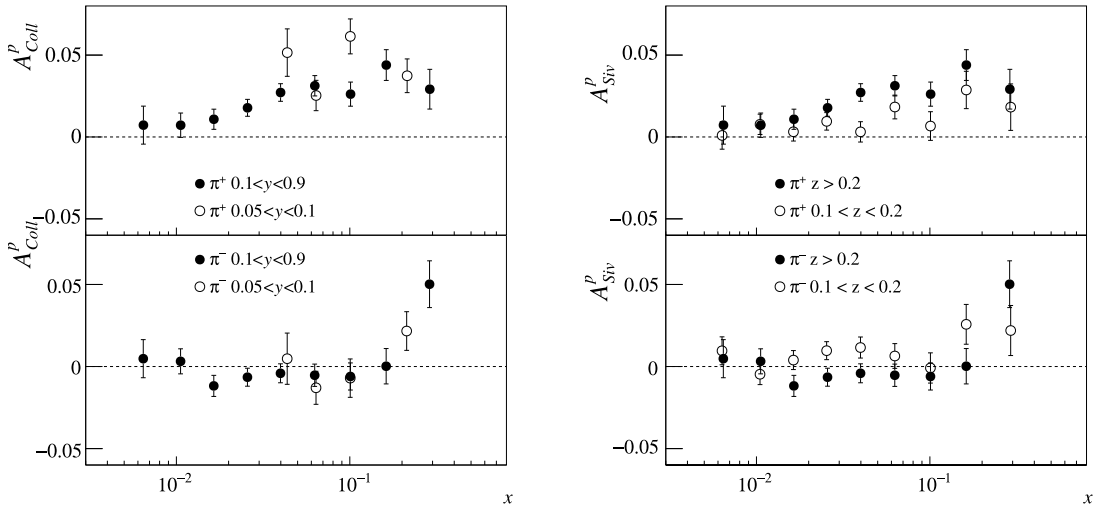

Fig. 13. The Sivers asymmetries for pions in different y ranges (left) and z ranges (right), 2010 data.

show smaller values. The comparison of the pion asymmetries as a function of x for the two separated z ranges are shown in the right panel of Fig. 13. For negative pions, a positive signal shows up in the low-z region, which is not observed for larger values of z.

In summary, using the high statistics data collected in 2007 and 2010, COMPASS has measured the Collins and Sivers asymmetries in muonproduction of charged pions and charged and neutral kaons produced off transversely polarised protons. The high energy muon beam allowed the measurement of a broad kinematic range in x and Q^2. The x, z and p_T dependences of the asymmetries were studied. Further investigations extending the range in z and y were also performed. The Collins asymmetries are definitely different from zero for pions and there are hints of a non-zero signal also for kaons, although in this case the statistical significance is marginal. The Sivers asymmetries are positive for positive pions and kaons, although different in size. This result is of particular interest since it can be used to access the sea quark Sivers PDFs. The results presented in this paper provide an important input for the global analyses. Together with other measurements covering complementary kinematic ranges, they allow the study of the Q^2 dependence of the asymmetries and the quantitative extraction of the Collins FF and of the transversity and Sivers PDFs. This information is crucial for the predictions for future Drell–Yan measurements and for measurements at future high-energy electron–ion colliders.

Acknowledgements

This work was made possible thanks to the financial support of our funding agencies. We also acknowledge the support of the CERN management and staff, as well as the skills and efforts of the technicians of the collaborating institutes.

References

[1] A. Kotzinian, Nucl. Phys. B 441 (1995) 234.
[2] P.J. Mulders, R.D. Tangerman, Nucl. Phys. B 461 (1996) 197;
P.J. Mulders, R.D. Tangerman, Nucl. Phys. B 484 (1997) 538 (Erratum).
[3] A. Bacchetta, et al., J. High Energy Phys. 0702 (2007) 093.
[4] A. Bacchetta, et al., Phys. Rev. D 70 (2004) 117504.
[5] J.C. Collins, Nucl. Phys. B 396 (1993) 161.
[6] D.W. Sivers, Phys. Rev. D 41 (1990) 83.
[7] E.S. Ageev, et al., COMPASS Collaboration, Nucl. Phys. B 765 (2007) 127.
[8] M. Alekseev, et al., COMPASS Collaboration, Phys. Lett. B 673 (2009) 127.
[9] M. Alekseev, et al., COMPASS Collaboration, Phys. Lett. B 692 (2010) 240.
[10] C. Adolph, et al., COMPASS Collaboration, Phys. Lett. B 717 (2012) 376.
[11] C. Adolph, et al., COMPASS Collaboration, Phys. Lett. B 717 (2012) 383.
[12] P. Abbon, et al., Nucl. Instrum. Methods Sect. A 616 (2010) 21.
[13] A. Airapetian, et al., HERMES Collaboration, Phys. Lett. B 693 (2010) 11.
[14] A. Airapetian, et al., HERMES Collaboration, Phys. Rev. Lett. 103 (2009) 152002.
[15] X. Qian, et al., Jefferson Lab Hall A Collaboration, Phys. Rev. Lett. 107 (2011) 072003.
[16] K. Allada, et al., Jefferson Lab Hall A Collaboration, Phys. Rev. C 89 (2014) 042201.
[17] Y.X. Zhao, et al., Jefferson Lab Hall A Collaboration, Phys. Rev. C 90 (5) (2014) 055201.
[18] P. Abbon, et al., COMPASS Collaboration, Nucl. Instrum. Methods Sect. A 577 (2007) 455.
[19] P. Abbon, et al., Nucl. Instrum. Methods Sect. A 631 (2011) 26.
[20] J. Beringer, et al., Particle Data Group, Phys. Rev. D 86 (2012) 010001.
[21] M. Diehl, S. Sapeta, Eur. Phys. J. C 41 (2005) 515, arXiv:hep-ph/0503023.
[22] M.G. Alekseev, et al., COMPASS Collaboration, Phys. Lett. B 690 (2010) 466.
[23] P. Amaudruz, et al., New Muon Collaboration, Nucl. Phys. B 371 (1992) 3.
[24] J. Ashman, et al., European Muon Collaboration, Z. Phys. C 57 (1993) 211.
[25] A.A. Akhundov, D.Yu. Bardin, L. Kalinovskaya, T. Riemann, Fortschr. Phys. 44 (1996) 373.
[26] M. Anselmino, et al., Phys. Rev. D 87 (2013) 094019.
[27] R. Seidl, et al., Belle Collaboration, Phys. Rev. D 86 (2012) 032011(E).
[28] A.V. Efremov, K. Goeke, P. Schweitzer, Eur. Phys. J. Spec. Top. 162 (2008) 1.
[29] A.V. Efremov, K. Goeke, P. Schweitzer, Czechoslov. J. Phys. 56 (2006) F181.
[30] M. Anselmino, et al., Eur. Phys. J. A 39 (2009) 89.
[31] M. Anselmino, E. Boglione, S. Melis, Phys. Rev. D 86 (2012) 014028.
[32] P. Sun, F. Yuan, Phys. Rev. D 88 (2013) 114012.
[33] M.G. Echevarria, et al., Phys. Rev. D 89 (2014) 074013.